



HAL
open science

Nonlinear modal properties of nonshallow cables

Walter Lacarbonara, Achille Paolone, Fabrizio Vestroni

► **To cite this version:**

Walter Lacarbonara, Achille Paolone, Fabrizio Vestroni. Nonlinear modal properties of nonshallow cables. *International Journal of Non-Linear Mechanics*, 2007, 42 (3), pp.542. 10.1016/j.ijnonlinmec.2007.02.013 . hal-00501748

HAL Id: hal-00501748

<https://hal.science/hal-00501748>

Submitted on 12 Jul 2010

HAL is a multi-disciplinary open access archive for the deposit and dissemination of scientific research documents, whether they are published or not. The documents may come from teaching and research institutions in France or abroad, or from public or private research centers.

L'archive ouverte pluridisciplinaire **HAL**, est destinée au dépôt et à la diffusion de documents scientifiques de niveau recherche, publiés ou non, émanant des établissements d'enseignement et de recherche français ou étrangers, des laboratoires publics ou privés.

Author's Accepted Manuscript

Nonlinear modal properties of nonshallow cables

Walter Lacarbonara, Achille Paolone, Fabrizio Vestroni

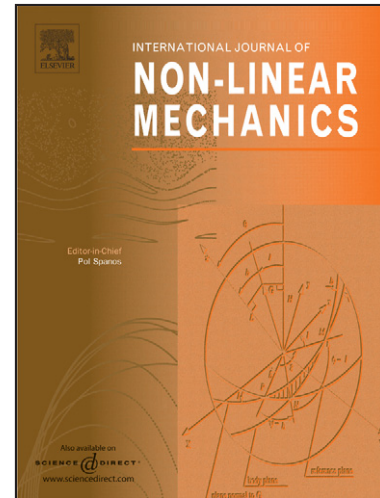
PII: S0020-7462(07)00062-5
DOI: doi:10.1016/j.ijnonlinmec.2007.02.013
Reference: NLM 1347

To appear in: *International Journal of Non-Linear Mechanics*

Received date: 29 March 2006
Revised date: 15 February 2007
Accepted date: 16 February 2007

Cite this article as: Walter Lacarbonara, Achille Paolone and Fabrizio Vestroni, Nonlinear modal properties of nonshallow cables, *International Journal of Non-Linear Mechanics* (2007), doi:10.1016/j.ijnonlinmec.2007.02.013

This is a PDF file of an unedited manuscript that has been accepted for publication. As a service to our customers we are providing this early version of the manuscript. The manuscript will undergo copyediting, typesetting, and review of the resulting galley proof before it is published in its final citable form. Please note that during the production process errors may be discovered which could affect the content, and all legal disclaimers that apply to the journal pertain.



www.elsevier.com/locate/nlm

NONLINEAR MODAL PROPERTIES OF NONSHALLOW CABLES

Walter Lacarbonara¹, Achille Paolone and Fabrizio Vestroni

Dipartimento di Ingegneria Strutturale e Geotecnica,

Università di Roma La Sapienza, via Eudossiana 18, Rome 00184 Italy

Running Title: *Nonlinear modes of nonshallow cables*

Total number of pages: 35

Total number of tables: 0

Total number of figures: 10

¹Author to whom all correspondence should be addressed

Nonlinear modal properties of nonshallow cables

Walter Lacarbonara, Achille Paolone and Fabrizio Vestroni

Dipartimento di Ingegneria Strutturale e Geotecnica,

Università di Roma La Sapienza,

via Eudossiana 18, Rome 00184 Italy

Abstract

A nonlinear mechanical model of nonshallow linearly elastic suspended cables is employed to investigate the nonlinear modal characteristics of the free planar motions. An asymptotic analysis of the equations of motion is carried out directly on the partial-differential equations overcoming the drawbacks of a discretization process. The direct asymptotic treatment delivers the approximation of the individual nonlinear normal modes. General properties about the nonlinearity of the in-plane modes of different type - geometric, elasto-static and elasto-dynamic - are unfolded. The spatial corrections to the considered linear mode shape caused by the quadratic geometric forces are investigated for modes belonging to the three mentioned classes. Moreover, the convergence of Galerkin reduced-order models is discussed and the influence of passive modes is highlighted.

Keywords: Nonshallow cables, nonlinear normal mode, direct method of multiple scales, reduced-order models.

1 Introduction

The linear and nonlinear dynamics of suspended elastic cables have received considerable attention due to their use in several applications in the fields of communications, electricity, mooring systems, transportation, and crane-operation systems. The linear vibration theory of suspended cables is attributed to the work of Irvine and Caughey [1], Irvine [2], and Triantafyllou and co-workers [3, 4]. The modal properties of shallow cables have been shown to depend on one elasto-geometric parameter, the so-called Irvine's parameter.

Free nonlinear vibrations were studied in [5, 6] to mention only a few works. Several studies dealt either theoretically or experimentally with harmonically forced oscillations both for the nonresonant and the resonant cases, the latter including a plethora of modal interactions. In particular, it has been demonstrated that the responses of shallow suspended cables near the first crossover exhibit complex behavior due to the presence of multiple internal resonances involving in-plane and out-of-plane modes. Examples include the coexistence of different types of periodic motions and the occurrence of quasiperiodic and chaotic oscillations [7]-[10].

The great majority of the works, especially those addressing nonlinear vibrations, deals with shallow cables described by approximate mechanical models based on the static condensation of the longitudinal dynamics. In particular, a characterization of the nonlinear normal modes of shallow cables has been addressed in [11, 12]. An extensive and updated review of the state of the art on shallow cables can be found in [10].

On the contrary, a few studies have addressed linear and nonlinear dynamic behaviors of nonshallow cables whereas nonshallow configurations may occur in a number of engineering applications such as in cables used for cable railways, transmission lines, mooring lines or tag-lines. Hence, there is a practical and theoretical interest in investigating nonshallow cable configurations and the leading dynamics around them.

In [13, 14], a nonlinear mechanical model of nonshallow cables, describing the fully coupled longitudinal and transverse dynamics, was presented. Therein, results of the investigations into the spectral properties of linear free vibrations around the catenary configurations were reported. Differently from shallow cables, whose linear dynamics depend solely on Irvine's parameter, it is shown that the linear vibration properties of nonshallow cables depend on two parameters separately regulating the cable elastic and geometric stiffnesses. Among other properties, it was also determined where, in parameter space, the three classes of modes appear, namely, geometric, elasto-static and elasto-dynamic modes which were already partly mentioned in [3]. It was demonstrated that the elastic modes belong to a complete sequence of symmetric and skew-symmetric stretching modes starting

from the lowest elasto-static stretching mode with nearly constant elongation. These modes are manifested in the neighborhood of the various crossovers - the well-known (elasto-static) lowest crossovers and the highlighted higher-order (elasto-dynamic) crossovers. Away from these crossovers, the modes are geometric modes, in the sense that they are prevalently governed by the geometric stiffness, and exhibit leading transverse displacements.

In this paper, the primary focus is on the effects of the geometric nonlinearity on the modal properties; in particular, the objective is to characterize the nonlinear properties of the individual in-plane modes with a clear effort towards unfolding general properties. Further, the a priori knowledge of the nonlinear modal properties is the basis for the prediction of the features of unimodal forced responses and interaction phenomena (the type of bifurcations, the possible routes to chaotic solutions,...).

The nonlinear partial-differential equations of motion and boundary conditions are recast in first-order form to make the employed asymptotic scheme suitable for higher-order approximations. Then, the asymptotic analysis of individual nonlinear normal modes is presented. The main results on the nonlinear characteristics of the modal motions are summarized. They mostly relate to the so-called effective nonlinearity coefficient of the considered mode which regulates the bending of the backbone and to the shape functions dictating the spatial corrections to the considered linear mode shape at second order. General conclusions are drawn about the nonlinear laws of the modes, depending on whether they are geometric, elasto-static or elasto-dynamic.

2 Equations of motion

We denote $(O, \mathbf{i}, \mathbf{j}, \mathbf{k})$ the orthonormal basis of a fixed inertial reference frame with origin in O (Fig. 1), let N_0^* and N^* describe the static axial force due to gravity in the initial configuration \mathcal{C}_0 and the incremental dynamic force arising in the change from the initial to the current configuration \mathcal{C} . Imposing the balance of linear and angular momentum yields

the equation of free undamped motions as

$$\frac{\partial [N_0^* (\mathbf{a} - \hat{\mathbf{a}}_0)]}{\partial x^*} + \frac{\partial (N^* \mathbf{a})}{\partial x^*} = m_0 \sec \theta_0 \frac{\partial^2 \mathbf{u}^*}{\partial t^{*2}} \quad (1)$$

where x^* indicates the horizontal coordinate along the fixed \mathbf{i} direction. In Eq. (1), m_0 is the mass per unit cable length in its initial configuration \mathcal{C}_0 lying in the (\mathbf{i}, \mathbf{j}) -plane - here expressed as $\hat{\mathbf{p}}_0^*(x^*) = x^* \mathbf{i} + y^*(x^*) \mathbf{j}$; \mathbf{u}^* is the displacement vector, henceforth conveniently decomposed as $\mathbf{u}^*(x^*, t^*) = \hat{\mathbf{u}}^* + w^* \mathbf{k}$ with $\hat{\mathbf{u}}^*$ being the in-plane displacement (i.e., lying in the (\mathbf{i}, \mathbf{j}) -plane); $\hat{\mathbf{a}}_0(x^*)$ is the unit tangential vector in \mathcal{C}_0 and $\theta_0(x^*)$ is the angle between $\hat{\mathbf{a}}_0$ and \mathbf{i} given by $\theta_0(x^*) = \arctan(dy^*/dx^*)$; \mathbf{a} is the unit vector tangent to the current configuration of the cable axis. Henceforth, the same notation will be employed throughout the manuscript, namely, lowercase bold italic letters indicate vectors in \mathbb{E}^3 , hatted lowercase bold italic letters denote vectors lying in the (\mathbf{i}, \mathbf{j}) -plane, and lowercase bold italic letters denote the corresponding algebraic vectors.

The cable axial dilatation associated with the deformation from \mathcal{C}_0 to \mathcal{C} is

$$\nu = \left| \frac{d\mathbf{p}^*}{ds^*} \right| = \cos \theta_0 \left| \frac{d\mathbf{p}^*}{dx^*} \right| = \cos \theta_0 \sqrt{(1 + u')^2 + (\tan \theta_0 + v')^2 + w'^2} \quad (2)$$

where $|\cdot|$ represents the magnitude of the vectorial argument and the prime indicates differentiation with respect to the nondimensional coordinate $x = \frac{x^*}{\ell}$, s^* is the arclength along the cable axis in \mathcal{C}_0 . Further, the displacement components are nondimensionalized as $u := \frac{u^*}{\ell}$, $v := \frac{v^*}{\ell}$, $w := \frac{w^*}{\ell}$. The unit vector in the current tangential direction is expressed as

$$\mathbf{a} := \frac{\mathbf{p}'}{|\mathbf{p}'|} \equiv \cos \theta_0 \frac{(1 + u') \mathbf{i} + (\tan \theta_0 + v') \mathbf{j} + w' \mathbf{k}}{\nu} \quad (3)$$

Due to the relatively high axial stiffness of typical engineering cables, the initial configuration of the cable, represented by the catenary, and the axial load are, respectively,

$$y(x) = \frac{1}{\gamma} \left[\cosh \frac{\gamma}{2} - \cosh \gamma \left(\frac{1}{2} - x \right) \right], \quad N_0(x) = \cosh \gamma \left(\frac{1}{2} - x \right) \quad (4)$$

where $y := \frac{y^*}{\ell}$, $\gamma := \frac{mg\ell}{H_0^*}$ is solution of the geometric compatibility condition $\sinh \left(\frac{\gamma}{2} \right) = \frac{\gamma}{2} \eta_0$ with $\eta_0 := \frac{L_0}{\ell}$, L_0 is the initial total length of the cable, $N_0(x) := \frac{N_0^*(x^*)}{H_0^*}$, and H_0^* is the

horizontal projection of N_0^* . The extensibility of the cable under its own weight is neglected as it is typically done for engineering cables [2] since the elastic elongation is indeed very small, hence, uninfluential on the static equilibrium. On the contrary, for cables with a low elastic stiffness relative to the geometric stiffness, the cable elastic deformation mode should be accounted for. This can be shown rigorously for an elastic cable subject to its own weight. The compatibility condition delivering the horizontal component of the equilibrium axial force is

$$\frac{\eta_0}{k} + \frac{2}{\gamma} \sinh^{-1} \left(\frac{\eta_0 \gamma}{2} \right) = 1 \quad (5)$$

where $k := \frac{EA_0}{H_0^*}$, E is Young's modulus of elasticity and A_0 is the area of the undeformed cable cross section. When k is sufficiently large, the equation reduces to that governing the catenary, obtained neglecting the cable elasticity.

A linear constitutive elastic law relating the incremental axial load to the axial strain is adopted in the form $N^* = EA_0(\nu - 1)$ where $\nu - 1 := e$ is the axial elongation. Introducing a suitable nondimensional time $t := \omega_c t^*$ with $\omega_c := \sqrt{\frac{H_0^*}{m_0 \ell^2}}$, and the nondimensional axial force $N := \frac{N^*}{H_0^*} = k(\nu - 1)$, the ensuing nondimensional equations of motion, in componential form, are then expressed as

$$\begin{aligned} (\sec \theta_0) \ddot{u} - \left\{ \frac{\cos \theta_0}{\nu} \left[N_0(u' - \nu + 1) + N(1 + u') \right] \right\}' &= 0 \\ (\sec \theta_0) \ddot{v} - \left\{ \frac{\cos \theta_0}{\nu} \left[N_0(v' - \tan \theta_0(\nu - 1)) + N(v' + \tan \theta_0) \right] \right\}' &= 0 \\ (\sec \theta_0) \ddot{w} - \left[(N_0 + N) \frac{\cos \theta_0}{\nu} w' \right]' &= 0 \end{aligned} \quad (6)$$

The equations of motion are supplemented with the boundary conditions $\mathbf{u}(0, t) = \mathbf{0}$ and $\mathbf{u}(1, t) = \mathbf{0}$, for a cable suspended from two supports at the same level (Fig. 1).

In [13, 14] it was shown that, differently from shallow cables as far as the linear dynamics are concerned, nonshallow cables are governed by two independent parameters, relating to the geometric and elastic stiffness, namely, γ and k or $\lambda := \gamma \sqrt{\frac{k}{\eta_e}}$ with $\eta_e := \int_0^1 \cos^3 \theta_0 dx$. In [14] it was shown that typical values of k for engineering cables are within the range $[10^3, 10^4]$.

3 Asymptotic analysis of individual nonlinear normal modes

An asymptotic approach is well-suited to characterize the nonlinear properties of the individual nonlinear normal modes of cables. This type of nonlinear analysis can not be pursued via standard numerical solution approaches such as those based on weak formulations (finite elements, weighted residuals) unless a good initial estimate of the nonlinear modes is available. When the individual nonlinear modal manifolds of a nonlinear unforced and undamped system are not known a priori, the numerical responses would be affected by many modes (in principle, all the modes captured by the numerical discretization). The ensuing numerical responses would not be helpful for disclosing the featured nonlinear behaviors of individual normal modes. Furthermore, the employed direct asymptotic expansion is the most accurate local solution approach since it does not discard any spatial information of the motion but it embodies all of it into the solutions of a few boundary-value problems at second order.

The cable motions are assumed to occur in the neighborhood of the initial configuration \mathcal{C}_0 and are such that the cable tension never vanishes. The cable responses are consequently described seeking the solutions of the following third-order Mac Laurin series expansion of the equation of motion:

$$\begin{aligned} \sec \theta_0 \ddot{\mathbf{u}} - [N^0 \mathbf{a}_1 + ke_1 \hat{\mathbf{a}}_0]' - [N^0 \mathbf{a}_2 + ke_2 \hat{\mathbf{a}}_0 + 2ke_1 \mathbf{a}_1]' \\ - [N^0 \mathbf{a}_3 + ke_3 \hat{\mathbf{a}}_0 + 3ke_2 \mathbf{a}_1 + 3ke_1 \mathbf{a}_2]' = \mathbf{0} \end{aligned} \quad (7)$$

where e_j and \mathbf{a}_j are the j th-order terms of e and \mathbf{a} , respectively. Letting $\mathbf{u} := (u, v, w)^\top$ and $\mathbf{v} := (\dot{u}, \dot{v}, \dot{w})^\top$ represent the algebraic vectors associated to the Euclidean displacement and velocity vectors, the ensuing equations can be cast as:

$$\begin{aligned} \dot{\mathbf{u}} - \mathbf{v} &= \mathbf{0} \\ \mathcal{I} \dot{\mathbf{v}} + \mathcal{L} \mathbf{u} &= \mathcal{N}_2(\mathbf{u}, \mathbf{u}) + \mathcal{N}_3(\mathbf{u}, \mathbf{u}, \mathbf{u}) \end{aligned} \quad (8)$$

along with the boundary conditions previously described.

In (8), $\mathcal{I} = (\sec \theta_0)(x) \mathbf{I}$ (\mathbf{I} is the identity tensor) and \mathcal{L} denote the inertial and linear elasto-geometric operators, respectively. Namely, $\mathcal{L} := \text{diag}[\hat{\mathcal{L}}, \mathcal{L}]$ due to the uncoupling

of the equations of motion where $\hat{\mathcal{L}}$ and \mathcal{L} denote the in-plane and out-of-plane stiffness operators, respectively (reported in [14]). On the other hand, the quadratic and cubic restoring forces, in operator form, are

$$\begin{aligned}\mathcal{N}_2(\mathbf{u}, \mathbf{u}) &= [N^0 \mathbf{a}_2(\mathbf{u}, \mathbf{u}) + k e_2(\mathbf{u}, \mathbf{u}) \hat{\mathbf{a}}_0 + 2k e_1(\mathbf{u}) \mathbf{a}_1(\mathbf{u})]' \\ \mathcal{N}_3(\mathbf{u}, \mathbf{u}, \mathbf{u}) &= [N^0 \mathbf{a}_3(\mathbf{u}, \mathbf{u}, \mathbf{u})]' \\ &\quad + [k e_3(\mathbf{u}, \mathbf{u}, \mathbf{u}) \hat{\mathbf{a}}_0 + 3k e_2(\mathbf{u}, \mathbf{u}) \mathbf{a}_1(\mathbf{u}) + 3k e_1(\mathbf{u}) \mathbf{a}_2(\mathbf{u}, \mathbf{u})]'\end{aligned}\tag{9}$$

Their componential forms are given in Appendix A. For computational reasons, it is worth noting that \mathcal{N}_2 is non-commutative, i.e., $\mathcal{N}_2(\mathbf{u}, \mathbf{w}) \neq \mathcal{N}_2(\mathbf{w}, \mathbf{u})$.

In the following, the analysis is first developed for individual planar modes, away from internal resonances. To this end, the ansatz on the form of the solutions of Eqs. (8) is

$$\hat{\mathbf{u}}(x, t) = \sum_{k=1}^3 \epsilon^k \hat{\mathbf{u}}_k(x, t_0, t_2) + \dots, \quad \hat{\mathbf{v}}(x, t) = \sum_{k=1}^3 \epsilon^k \hat{\mathbf{v}}_k(x, t_0, t_2) + \dots\tag{10}$$

where $\hat{\mathbf{u}} := (u, v)^\top$, $\hat{\mathbf{v}} := (\dot{u}, \dot{v})^\top$ are the restrictions of the displacement \mathbf{u} and velocity \mathbf{v} to the (i, j) -plane, $t_0 := t$ is the fast time scale, $t_2 := \epsilon^2 t$ is the stretched time scale, and ϵ is a small dimensionless number introduced to measure the order of magnitude of the deviations from the initial configuration \mathcal{C}_0 . Then, the first derivative with respect to time is defined as $\partial/\partial t = D_0 + \epsilon^2 D_2 + \dots$ where $D_k := \partial/\partial t_k$. The solution is considered independent of the slow time scale $t_1 = \epsilon t$ because no resonant terms arise at second order away from 2:1 internal resonances.

Substituting (10) into the system of first-order (in time) equations of motion and boundary conditions, using the independence of the time scales, and equating coefficients of like powers of ϵ yields

Order ϵ :

$$\begin{aligned}D_0 \hat{\mathbf{u}}_1 - \hat{\mathbf{v}}_1 &= \mathbf{0} \\ \hat{\mathcal{I}}(D_0 \hat{\mathbf{v}}_1) + \hat{\mathcal{L}} \hat{\mathbf{u}}_1 &= \mathbf{0}\end{aligned}\tag{11}$$

Order ϵ^2 :

$$\begin{aligned} D_0 \hat{\mathbf{u}}_2 - \hat{\mathbf{v}}_2 &= \mathbf{0} \\ \hat{\mathcal{I}}(D_0 \hat{\mathbf{v}}_2) + \hat{\mathcal{L}} \hat{\mathbf{u}}_2 &= \hat{\mathcal{N}}_2(\hat{\mathbf{u}}_1, \hat{\mathbf{u}}_1) \end{aligned} \quad (12)$$

Order ϵ^3 :

$$\begin{aligned} D_0 \hat{\mathbf{u}}_3 - \hat{\mathbf{v}}_3 &= -D_2 \hat{\mathbf{u}}_1 \\ \hat{\mathcal{I}}(D_0 \hat{\mathbf{v}}_3) + \hat{\mathcal{L}} \hat{\mathbf{u}}_3 &= -D_2 \hat{\mathbf{v}}_1 + \hat{\mathcal{N}}_2(\hat{\mathbf{u}}_1, \hat{\mathbf{u}}_2) + \hat{\mathcal{N}}_2(\hat{\mathbf{u}}_2, \hat{\mathbf{u}}_1) + \hat{\mathcal{N}}_3(\hat{\mathbf{u}}_1, \hat{\mathbf{u}}_1, \hat{\mathbf{u}}_1) \end{aligned} \quad (13)$$

where $\hat{\mathcal{N}}_2$ and $\hat{\mathcal{N}}_3$ denote the restrictions of the quadratic and cubic forces to the (i, j) -plane, and we further note that use of the non-commutativity of $\hat{\mathcal{N}}_2$ was made.

Because the considered mode is away from internal resonances with other modes, the solution at order ϵ can be assumed as

$$\hat{\mathbf{u}}_1 = A_m(t_2) e^{i\omega_m t_0} \phi_m(x) + cc, \quad \hat{\mathbf{v}}_1 = i\omega_m A_m(t_2) e^{i\omega_m t_0} \phi_m(x) + cc \quad (14)$$

where ω_m is the linear eigenfrequency of the m th in-plane mode; $i := \sqrt{-1}$, and $A_m \in \mathbb{C}$ is the complex-valued amplitude of the mode at leading order; cc denotes the complex conjugate of the preceding terms. Substituting (14) into the second-order problem, Eq. (12), yields

$$\begin{aligned} D_0 \hat{\mathbf{u}}_2 - \hat{\mathbf{v}}_2 &= \mathbf{0} \\ \hat{\mathcal{I}}(D_0 \hat{\mathbf{v}}_2) + \hat{\mathcal{L}} \hat{\mathbf{u}}_2 &= (A_m^2 e^{2i\omega_m t_0} + A_m \bar{A}_m) \hat{\mathbf{Q}}(x) + cc \end{aligned} \quad (15)$$

where the bar indicates the complex conjugate and $\hat{\mathbf{Q}}(x) := \hat{\mathcal{N}}_2(\phi_m, \phi_m)$. The particular solution of the second-order problem can be expressed as

$$\begin{aligned} \hat{\mathbf{u}}_2 &= A_m^2 e^{2i\omega_m t_0} \Phi^{(\infty)}(x) + A_m \bar{A}_m \Psi^{(\infty)}(x) + cc \\ \hat{\mathbf{v}}_2 &= 2i\omega_m \Phi^{(\infty)}(x) A_m^2 e^{2i\omega_m t_0} + cc \end{aligned} \quad (16)$$

where the functions $\Phi^{(\infty)}$ and $\Psi^{(\infty)}$ are solutions of the following boundary-value problems:

$$\hat{\mathcal{L}}(x) \Phi^{(\infty)}(x) - 4\omega_m^2 \mathcal{I}(x) \Phi^{(\infty)}(x) = \hat{\mathbf{Q}}(x), \quad \hat{\mathcal{L}}(x) \Psi^{(\infty)}(x) = \hat{\mathbf{Q}}(x) \quad (17)$$

where, for sake of clarity, the space-dependence of the inertial and stiffness operators has been made explicit. The boundary conditions are $\Phi^{(\infty)}(0) = \mathbf{0}$ and $\Phi^{(\infty)}(1) = \mathbf{0}$, $\Psi^{(\infty)}(0) = \mathbf{0}$ and $\Psi^{(\infty)}(1) = \mathbf{0}$.

Since the inertial and stiffness operators depend on the position coordinate x , closed-form solutions of (17) do not exist in general. However, the solutions can be conveniently expressed in series form in terms of the eigenfunctions as follows:

$$\Phi^{(\infty)}(x) = \sum_{j=1}^{\infty} \alpha_j \phi_j(x), \quad \Psi^{(\infty)}(x) = \sum_{j=1}^{\infty} \beta_j \phi_j(x) \quad (18)$$

where

$$\alpha_j := \frac{1}{[(\omega_j)^2 - 4(\omega_m)^2]} \left(\int_0^1 \phi_j(x) \cdot \hat{\mathbf{Q}}(x) dx \right), \quad \beta_j := \frac{1}{(\omega_j)^2} \left(\int_0^1 \phi_j(x) \cdot \hat{\mathbf{Q}}(x) dx \right) \quad (19)$$

and the dot indicates the standard inner product. We observe that the coefficient in Eq. (19)₁ diverges when $\omega_j = 2\omega_m$, hence the displacement would grow indefinitely large, due to the fact that a two-to-one internal resonance between the j th and m th mode may be activated and the expansion based on the individual mode breaks down. In this case, a two-mode expansion is necessary to properly account for the interaction as it is discussed further on.

Substituting Eq. (16) into the third-order problem and imposing the solvability condition [18] at this order yields the following modulation equation:

$$\frac{i}{4} \dot{A}_m = \Gamma^{(\infty)} A_m^2 \bar{A}_m \quad (20)$$

The *effective nonlinearity coefficient* $\Gamma^{(\infty)}$ regulates the bending of the backbone of the cable oscillating in the m th mode, that is, the nonlinear frequency variation with the amplitude

$$\omega_m^{(\infty)} := \omega_m - \Gamma^{(\infty)} a_m^2 \quad (21)$$

The coefficient can be regarded as a nonlinear modal constitutive parameter embodying the combined modal effects of the quadratic and cubic forces as it is given by

$$\begin{aligned} \Gamma^{(\infty)} &:= \Gamma_2^{(\infty)} + \Gamma_3, \quad \Gamma_2^{(\infty)} := \frac{1}{8\omega_m} \int_0^1 \phi_m(x) \cdot \mathbf{F}_2^{(\infty)}(x) dx, \\ \Gamma_3 &:= \frac{1}{8\omega_m} \int_0^1 \phi_m(x) \cdot \mathbf{F}_3(x) dx \end{aligned} \quad (22)$$

The vectors $\mathbf{F}_2^{(\infty)}(x)$ and $\mathbf{F}_3(x)$ represent the resonant geometric forces at third order arising from the overall quadratic and cubic nonlinear forces, respectively, and are expressed as

$$\begin{aligned}\mathbf{F}_2^{(\infty)}(x) &:= \hat{\mathcal{N}}_2(\Phi^{(\infty)}, \phi_m) + \hat{\mathcal{N}}_2(\phi_m, \Phi^{(\infty)}) + 2\hat{\mathcal{N}}_2(\Psi^{(\infty)}, \phi_m) + 2\hat{\mathcal{N}}_2(\phi_m, \Psi^{(\infty)}) \\ \mathbf{F}_3(x) &:= 3\hat{\mathcal{N}}_3(\phi_m, \phi_m, \phi_m)\end{aligned}\quad (23)$$

In Eq. (22), $\Gamma_2^{(\infty)}$ denotes the softening-type contribution of the quadratic forces which, in principle, depends - through the second-order functions $\Phi^{(\infty)}$ and $\Psi^{(\infty)}$ - on all of the cable eigenfunctions as emphasized by the superscript ∞ , whereas Γ_3 is the hardening-type contribution of the cubic forces depending only on the considered active mode ([18], [16]).

The second-order functions regulate the spatial corrections to the linear mode shape ϕ_m in the displacement field

$$\begin{aligned}\hat{\mathbf{u}}^{(\infty)}(x, t) &= a_m \cos(\omega_m^{(\infty)}t + \psi_m)\phi_m(x) \\ &+ \frac{a_m^2}{2} \left[\cos(2(\omega_m^{(\infty)}t + \psi_m))\Phi^{(\infty)}(x) + \Psi^{(\infty)}(x) \right]\end{aligned}\quad (24)$$

where ψ_m is a constant. It is clear that the cable oscillates with frequency $\omega_m^{(\infty)}$ around the displaced configuration given by $\hat{\mathbf{p}} = \hat{\mathbf{p}}_0 + 1/2 a_m^2 \Psi^{(\infty)}(x)$. As it was pointed out in [9], the calculated individual nonlinear normal modes are not synchronous and, hence, do not possess all the features of the original definition given by Rosenberg [19].

Instead of the direct perturbation approach, we can employ a full-basis Galerkin discretization, $\hat{\mathbf{u}}(x, t) = \sum_{j=1}^{\infty} q_j(t)\phi_j(x)$, and, subsequently, the method of multiple scales may be applied to the resulting infinite-dimensional set of ODE's. It turns out that the cubic part of the effective nonlinearity coefficient is the same as in Eq. (22) whereas the contribution from the quadratic forces is expressed as [16]

$$\begin{aligned}\Gamma_2^{(\infty)} &= \sum_{j=1}^{\infty} S_j, \quad S_j = \frac{1}{8\omega_m} \left[(\Lambda_{mmj} + \Lambda_{mjm}) \left(\frac{2\Lambda_{jmm}}{\omega_j^2} + \frac{\Lambda_{jmm}}{\omega_j^2 - 4\omega_m^2} \right) \right], \\ \Lambda_{jkh} &:= \int_0^1 \phi_j \cdot \hat{\mathcal{N}}_2(\phi_k, \phi_h) dx\end{aligned}\quad (25)$$

In agreement with our previous observation, the coefficient in Eq. (25) diverges when $\omega_j = 2\omega_m$ due to a 2:1 internal resonance between the j th and m th mode. To account for

the 2:1 interaction, the generating solution must include the two interacting modes and a third-order expansion has to be pursued. The expansion was obtained for a general system with quadratic and cubic nonlinearities in [11]. Here, we summarize only the modulation equations governing the slow variations of the amplitudes and phases of the two interacting modes; that is,

$$\begin{aligned}\frac{i}{4}\dot{A}_m &= \frac{1}{8\omega_m}(\Lambda_{mmm} + \Lambda_{mnm})A_n\bar{A}_m e^{i\delta t} + \hat{\Gamma}^\infty A_m^2\bar{A}_m + \frac{1}{8\omega_m}\hat{\Gamma}_{mn}^\infty A_m A_n \bar{A}_n \\ \frac{i}{4}\dot{A}_n &= \frac{1}{8\omega_n}\Lambda_{nmm}A_m^2 e^{-i\delta t} + \hat{\Delta}^\infty A_n^2\bar{A}_n + \frac{1}{8\omega_n}\hat{\Gamma}_{mn}^\infty A_n A_m \bar{A}_m\end{aligned}\quad (26)$$

where A_m and A_n are the complex-valued amplitudes of the interacting modes at first order, δ is a small parameter expressing the detuning of the internal resonance, $\omega_n = 2\omega_m + \delta$. The softening part of the nonlinearity coefficient of the m th mode, Eq. (25), is modified as follows in the presence of the 2:1 resonance: the summation does not include the n th term (i.e., the term corresponding to the high-frequency mode) which, on the contrary, is $9/(4\omega_n^2)\Lambda_{nmm}(\Lambda_{mmm} + \Lambda_{mnm})/(8\omega_m)$. Here and henceforth, the modified coefficient will be denoted $\hat{\Gamma}^{(\infty)}$. The other coefficients appearing in Eq. (26) are given in Appendix B.

On the other hand, when a truncation to the lowest M modes is performed, a reduced-order model yields an effective nonlinearity coefficient given by

$$\Gamma^M = \sum_{j=1}^M S_j + \Gamma_3 \quad (27)$$

and, in turn, the nonlinear frequency is $\omega_m^M := \omega_m - \Gamma^M a_m^2$.

3.1 Limits of validity of the no-compression cable model

The adopted cable model does not account for the fact that, when the tensile force vanishes, the cable can not resist compression. Several studies have addressed the effect of cable loosening on nonlinear vibrations of shallow cables [20]. Here, we are interested in calculating the amplitude range of validity of the no-compression cable model. To this end, the elongation, to within second order, is expressed as

$$e_m(x, t) = a_m \cos \varphi_m(t) \mathcal{Y}_1(x) + a_m^2 [\cos 2\varphi_m(t) \mathcal{Y}_2(x) + \mathcal{Y}_3(x)] \quad (28)$$

where $\varphi_m(t) := \omega_m^{(\infty)}t + \psi_m$

$$\begin{aligned}\Upsilon_1(x) &= \cos \theta_0^2 \left[\phi'_{1(m)} + \tan \theta_0 \phi'_{2(m)} \right] \\ \Upsilon_2(x) &= \frac{1}{2} \cos \theta_0^2 \left\{ \Phi'_1 + \tan \theta_0 \Phi'_2 + \frac{1}{2} \cos \theta_0^2 \left[\phi'_{1(m)} - \tan \theta_0 \phi'_{2(m)} \right]^2 \right\} \\ \Upsilon_3(x) &= \frac{1}{2} \cos \theta_0^2 \left\{ \Psi'_1 + \tan \theta_0 \Psi'_2 + \frac{1}{2} \cos \theta_0^2 \left[\phi'_{1(m)} - \tan \theta_0 \phi'_{2(m)} \right]^2 \right\}\end{aligned}\quad (29)$$

Here, $\phi_{j(m)}$ ($j = 1, 2$) indicates the j th component of the m th mode, Φ_j and Ψ_j are the j th components of the functions $\Phi^{(\infty)}$ and $\Psi^{(\infty)}$, respectively. Then, the total nondimensional tension is

$$\hat{N}(x, t; a_m) = N_0(x) + k e_m(x, t; a_m) \quad (30)$$

The tension is assumed to attain the minimum when the modal elongation attains its maximum (i.e., the elastic cable shortening $e_m = \nu_m - 1$ is maximum) at x_m (e.g., $x_m = \frac{1}{2}$ or $\frac{1}{4}$ for the first symmetric and skew-symmetric modes, respectively). Hence, $\hat{N}(x_m, t; a) =: \check{N}(t; a_m)$ becomes a function of time t and the amplitude a_m at the natural frequency. To determine the minimum of $\check{N}(t; a_m)$, the extremal values of $\check{e}_m := e_m(x_m, t; a_m)$ are sought. They are obtained when (i) $\sin \varphi_m(t) = 0$ or (ii) $\cos \varphi_m(t) = -\check{\Upsilon}_1 / (4a_m \check{\Upsilon}_2)$ where $\check{\Upsilon}_j := \Upsilon_j(x_m)$. In the first case,

$$\check{e}_m = \pm a_m \check{\Upsilon}_1 + a_m^2 (\check{\Upsilon}_2 + \check{\Upsilon}_3) \quad (31)$$

and the amplitude that makes $\check{N}(a)$ vanish is

$$a_m = 1/2 \left[\pm \check{\Upsilon}_1 \pm \sqrt{(\check{\Upsilon}_1)^2 - 4/k \check{N}_0 (\check{\Upsilon}_2 + \check{\Upsilon}_3)} \right] (\check{\Upsilon}_2 + \check{\Upsilon}_3)^{-1} \quad (32)$$

provided that $\check{\Upsilon}_1^2 \geq 4/k |\check{N}_0 (\check{\Upsilon}_2 + \check{\Upsilon}_3)|$. In case (ii),

$$\check{e}_m = a_m^2 (\check{\Upsilon}_3 - \check{\Upsilon}_2) \check{\Upsilon}_2 - \frac{\check{\Upsilon}_1^2}{8} \quad (33)$$

and the amplitude where $\check{N}(a)$ vanishes is

$$a_m = \sqrt{\left(\frac{\check{\Upsilon}_1^2}{8\check{\Upsilon}_2} - \check{N}_0 \right) (\check{\Upsilon}_3 - \check{\Upsilon}_2)^{-1}} \quad (34)$$

provided that the argument of the square root be greater than zero. Consequently, the admissible upper bound of the amplitude for maintaining positive tension in the cable is the minimum of the positive values expressed by Eqs. (32) and (34).

4 Nonlinear modal motions

The nonlinear properties of the individual modes are investigated with specific efforts towards unfolding general properties. Besides regulating the system free nonlinear oscillations, these nonlinear modal properties allow also to predict the features of the unimodal forced responses or interactions. The nonlinear laws of the modes, as discussed in the preceding section, are dictated by the effective nonlinearity coefficient $\Gamma^{(\infty)}$. Its investigation is conducted under different static regimes and for different cable parameters generalizing previous results on shallow cables. Further, the convergence of the effective nonlinearity coefficient is studied outlining the reliability of low-dimensional Galerkin-reduced models. Thereafter, the nonlinear modifications of the modal motions are discussed.

4.1 The nonlinearity of the individual normal modes

The effective nonlinearity coefficient of low-order modes belonging to the three classes of modes are considered; namely, geometric, elasto-static and elasto-dynamic modes. In the (γ, λ) -plane (Fig. 2b), we consider three regions corresponding to three principal static regimes [14]: $\gamma \in [0, 0.5]$ is the region of shallow profiles (the dark grey region in Fig. 2b) whereas $\gamma > 1$ is identified with the region of nonshallow profiles (the lightly shaded region in Fig. 2b). The interposed region, $\gamma \in [0.5, 1]$, is a transition region between the two static regimes where the cable is considered as being neither shallow nor nonshallow. These regions ensue from appreciating how the sag-to-span ratio d varies with γ (Fig. 2a). Further, in Fig. 2b, the region of admissible elastic stiffness k in the (γ, λ) -plane is shown. The iso-stiffness curves are drawn according to the definition of Irvine's parameter. The two lateral thick curves denote the boundaries of the admissible region and correspond to $k_1 = 5 \cdot 10^2$ and $k_3 = 5 \cdot 10^4$, respectively. In Figs. 2c and 2d, the frequencies of the transition cables with $\gamma = 0.75$ and those of nonshallow cables with $\gamma = 1.5$ are shown, respectively. The shaded area denotes regions of non physically admissible cable parameters.

The nonlinear characteristics of the modal properties are discussed considering variations of the effective nonlinearity coefficient with Irvine's parameter λ and fixed values

of the geometric flexibility parameter γ . In the following, the modes of two representative cases are considered, namely, the transition regime ($\gamma = 0.75$) and the nonshallow regime ($\gamma = 1.5$). Previous results relating to shallow cables [12, 15] have shown that the lowest mode is initially hardening ($\Gamma < 0$), then it becomes softening ($\Gamma > 0$) around its crossover and then hardening again before diverging due to a 2:1 resonance with the third symmetric mode. In Fig. 3, the effective nonlinearity coefficient of the lowest mode of the transition cables is shown. The mode $m = 1$ is a skew-symmetric geometric mode with two half-waves. The thick lines denote the coefficients $\Gamma^{(\infty)}$ and $\hat{\Gamma}^{(\infty)}$ obtained with the individual mode assumption and considering the 2:1 internal resonance (thicker line); the dashed line indicates the coefficient $\Gamma^{(m)}$ obtained with the one-mode discretization, retaining in Eq. (25) only the m th active linear mode. The coefficient $\Gamma^{(\infty)}$ indicates a hardening mode almost everywhere except for a region where a 2:1 internal resonance between the third mode ($m = 3$) and the considered first mode is activated around $\lambda \approx 3.9\pi$ and the coefficient of the individual mode consequently diverges. However, the coefficient $\hat{\Gamma}^{(\infty)}$ indicates that the mode preserves its hardening nature. The one-mode discretization captures the qualitative character of the mode although it greatly overestimates the nonlinear modal stiffness for higher λ .

In Fig. 4, the nonlinearity of the second symmetric mode ($m = 3$) of the transition cables is investigated. This mode undergoes a crossover with the second skew-symmetric mode for λ slightly below 4π where the mode becomes elasto-static. For low values of λ the mode is slightly hardening, thereafter around the crossover it becomes softening. There are divergences for 2:1 internal resonances between the considered mode and the seventh or ninth modes, respectively, occurring in a very narrow parameter range. Further increasing λ , the mode (above the crossover, $m = 4$) becomes hardening again with a strong divergence in the region around the 2:1 internal resonance with the ninth mode. The coefficient $\hat{\Gamma}^{(\infty)}$ accounting for the interaction is always negative indicating a hardening behavior. In the interaction region, there occurs a crossover between the frequencies of the ninth and the tenth mode indicating that the ninth mode is elasto-static. The nonlinearity

of the considered mode ($m = 3$) decreases significantly due to the softening contribution delivered by the coupled high-frequency elasto-static mode.

Then, the nonshallow regime, $\gamma = 1.5$, is investigated in the lowest symmetric modes; namely, the third symmetric mode, $m = 5$ (Fig. 5), the fourth symmetric mode, $m = 7$ (Fig. 6a), and the ninth symmetric mode, $m = 17$ (Fig. 6b). The third symmetric mode (Fig. 5) is hardening in the whole range except for the region where it becomes elasto-static around $\lambda = 5.7\pi$ while undergoing a crossover with the third skew-symmetric mode. In Fig. 6a, the nonlinearity of the fourth symmetric mode predicted with $\Gamma^{(\infty)}$ follows the same pattern as that of the second symmetric mode of the transition cable; it is hardening, then around the crossover it becomes softening, then hardening again and diverges due a 2:1 resonance with the ninth symmetric mode ($n = 17$). In this case, $\hat{\Gamma}^{(\infty)}$ indicates that, in the interaction region, the mode is hardening then softening with a change of curvature occurring where the interacting mode undergoes a crossover. Away from the resonance region, the mode regains its hardening signature. As shown in Fig. 6b, the high-frequency interacting mode is hardening except for the region where it undergoes the crossover thus attaining its peak elasto-static strain energy; hence, its softening contribution to the low-frequency coupled mode renders this mode softening while engaged in the interaction.

Finally, it is of interest to investigate the lowest elasto-dynamic mode exhibited by the nonshallow cable, with $\gamma = 1.5$. The considered mode is the seventeenth and its effective nonlinearity coefficient variation is shown in Fig. 7. This mode is hardening except for the region around its crossover with the eighteenth mode where it appears to be softening. This region corresponds to that where the mode becomes elasto-dynamic possessing a longitudinal motion much larger than the transverse component as shown in the modal displacements for $\lambda = 6.81\pi$ (right below the elasto-dynamic crossover). On the other hand, the mode is predicted as hardening with the one-mode discretization where it is indeed softening. However, where the coefficient becomes nearly vanishing, the one-mode discretization suggests the need of more passive modes in the discretization.

4.2 Spatial characteristics of the nonlinear modal motions

In this section, the quadratic spatial corrections to the active linear mode shape are discussed with the aim of quantifying the extent of its influence and the spectral content of these nonlinear corrections.

The displacement field at the instant of time when the velocity field vanishes takes the form (24) with $\cos \varphi_m(t) = \cos 2\varphi_m(t) \equiv 1$. In Fig. 8, the lowest (first skew-symmetric) mode of a nonshallow cable, when $\gamma = 1.5$ and $\lambda = 7\pi$, is considered. The u and v displacement components of the first- and second-order approximations are shown in parts (a) and (b), respectively, with the amplitude corresponding to the maximum admissible value (such that the corresponding motion maintains non-negative tension in the cable). It can be observed that the quadratic nonlinearities introduce appreciable spatial distortion into the shape of the leading motion making the horizontal symmetric and the vertical skew-symmetric displacement components neither symmetric nor skew-symmetric. To gain more insight into the characteristics of the motion, the modal coefficient α_k in $\Phi^{(\infty)}$ and the function itself, and the coefficient β_k and $\Psi^{(\infty)}$ are shown in parts (c) and (d), respectively. The considered skew-symmetric mode generates symmetric quadratic forces, hence, contributions from the even (symmetric) modes only are expected. However, besides the second, fourth and sixth mode shapes, there is a meaningful contribution of the seventh mode shape and minor contributions of the ninth and eleventh modes. The leading contributing modes, namely the sixth and seventh modes, are on the ramping parts of the $\omega_n - \lambda$ curves (see Fig. 2d), where, they turn out to be both symmetric elasto-static modes thus breaking down the natural sequence of symmetric and skew-symmetric modes as illustrated in [14]. In Fig. 9, we show how these signatures reflect themselves onto the convergence of the effective nonlinearity coefficient. As expected, the main contribution to the softening part of the effective nonlinearity coefficient comes from the two elasto-static modes, the sixth and seventh modes. The symmetric quadratic forces generate stretching of the cable axis which is almost entirely captured by the lowest symmetric elasto-static modes.

In Fig. 10, again the displacement field of the lowest mode (skew-symmetric) is shown

along with the coefficients α_k (and $\Phi^{(\infty)}$) and β_k (and $\Psi^{(\infty)}$) when $\gamma = 1.5$ and $\lambda = 12.6\pi$. In this case, although with the same sag-to-span ratio, the cable possesses a higher axial elastic stiffness. Besides the second mode, all of the even modes up to, and including the twelfth mode, contribute although a remarkable contribution comes from the twelfth and thirteenth modes. The reason for this participation is the same as in the previous case; that is, the twelfth and thirteenth modes are the lowest two elasto-static symmetric modes. Similarly, these modes determine the convergence of the effective nonlinearity coefficient.

5 Concluding remarks

A mechanical model describing finite motions of nonshallow cables around their initial catenary configurations has been employed to investigate the nonlinear vibration characteristics of individual in-plane modes. An asymptotic treatment based on the method of multiple scales has been applied directly to the partial-differential equations of motion and boundary conditions, overcoming the drawbacks of a discretization process.

The nonlinear characteristics of the modes of different type have been studied, namely, those relating to geometric modes (with prevalent transverse motion and negligible stretching), elasto-static modes (with prevalent transverse motion and appreciable stretching), elasto-dynamic modes (with prevalent longitudinal motion and stretching).

The general results about the investigated nonshallow cables, in line with known results on shallow cables, indicate that the geometric modes are hardening. Conversely, in the neighborhood of the localized regions where the frequencies undergo crossovers, the modes suffer a transition into elasto-static or elasto-dynamic modes; this transition, occurring within the linear eigenvalue structure, further makes the nonlinear mode of the softening-type. The physical phenomenon inherent in the change of the nonlinearity may be explained accounting for the fact that the relevant mode, around the crossovers, exhibits a shape with an appreciable transverse displacement inducing stretching which is quite sensitive to the upward or downward displacement directions. Indeed, a significant drift is caused by the quadratic geometric forces towards the upper configurations where the tension in the cable

can vanish thus leading to unsymmetrical softening behavior.

Moreover, the nonlinear shape modifications of the modal motions have been studied with a particular attention on the modal spatial content. It was found that quadratic modal forces involve modes with stretching, hence those modes that belong to the family of elastostatic modes whose frequency locus unfolds along the successive lowest crossovers. From the convergence analysis, the contribution of these modes was shown to be important; therefore, they must be included in the nonlinear description by reduced-order models, although they are far from the considered individual modes.

The issues pointed out about the suitability of reduced-order models of nonshallow cables are felt to be general and applicable also to those systems possessing stiffnesses/strain energies of different type and different orders of magnitude such as arches, membranes and shells.

Acknowledgment

This work was partially supported under a FY 2005-2006 PRIN Grant from the Italian Ministry of Education, University and Scientific Research.

References

- [1] Irvine, H. M. and Caughey, T. K., The linear theory of free vibrations of a suspended cable, *Proceedings of the Royal Society of London, Series A* **341** (1974) 299–315.
- [2] Irvine, H.M., *Cable Structures*, Dover Publications Inc., New York (1984).
- [3] Burgess, J.J., Triantafyllou, M.S., The elastic frequencies of cables, *Journal of Sound and Vibration* **120** (1988) 153–165.
- [4] Triantafyllou, M.S., The dynamics of taut inclined cables, *Quarterly Journal of Mechanics and Applied Mathematics* **37** (1984) 421–440.

- [5] Luongo, A., Rega, G., and Vestroni, F., Planar non-linear free vibrations of an elastic cable, *International Journal of Non-Linear Mechanics* **19** (1984) 39–52.
- [6] Cheng, S.-P. and Perkins, N. C., Closed-form vibration analysis of sagged cable/mass suspensions, *Journal of Applied Mechanics* **59** (1992) 923–928.
- [7] Lee, C. L. and Perkins, N. C., Three-dimensional oscillations of suspended cables involving simultaneous internal resonances, *Nonlinear Dynamics* **8** (1995) 45–63.
- [8] Nayfeh, A. H., Arafat, H., Chin, C. M., and Lacarbonara, W., Multimode interactions in suspended cables, *Journal of Vibration and Control* **8** (2002) 337–387.
- [9] Nayfeh A. H., Nayfeh, S. A., Nonlinear normal modes of a continuous system with quadratic nonlinearities, *Journal of Vibration and Acoustics* **117** (1995) 129–136.
- [10] Rega, G., Nonlinear vibrations of suspended cables - Part I: Modeling and analysis. Part II: Deterministic phenomena, *Applied Mechanics Review* **57** (2004) 443–479.
- [11] Lacarbonara, W., Rega, G., Nayfeh A. H., Resonant non-linear normal modes. Part I: analytical treatment for structural one-dimensional systems, *International Journal of Non-Linear Mechanics* **38** (2003) 851–872.
- [12] Arafat, H. N., and Nayfeh, A. H., Non-linear responses of suspended cables to primary resonance excitations, *Journal of Sound and Vibration* **266** (2003) 325–354.
- [13] Lacarbonara, W., Paolone, A., Vestroni, F., Shallow versus nonshallow cables: linear and nonlinear vibration performance, in *Proceedings of the Fifth EUROMECH Non-linear Dynamics Conference*, Eindhoven, The Netherlands, August 7-12, 2005.
- [14] Lacarbonara, W., Paolone, A., Vestroni, F., Elastodynamics of nonshallow suspended cables: Linear modal properties, *Journal of Vibration and Acoustics*, (2007) in press.
- [15] Rega, G., Lacarbonara, W., and Nayfeh, A. H., 2000, Reduction methods for nonlinear vibrations of spatially continuous systems with initial curvature, in *Solid Mechanics and Its Applications* **77**, Kluwer (2000) 235.

- [16] Lacarbonara, W., Direct treatment and discretizations of nonlinear spatially continuous systems, *Journal of Sound and Vibration* **221** (1999) 849–866.
- [17] Antman, S.S., *Nonlinear problems of elasticity* (2005) Springer-Verlag, New York.
- [18] Nayfeh, A. H., Lacarbonara, W. On the discretization of spatially continuous systems with quadratic and cubic nonlinearities, *JSME International Journal* **41** (1998) 510-531.
- [19] Rosenberg, R. M., On nonlinear vibrations of systems with many degrees of freedom, *Advances in Applied Mechanics* **9** (1966) 155-242.
- [20] Wu, Q., Takahashi, K., Nakamura, S. Nonlinear response of cables subjected to periodic support excitation considering cable loosening, *Journal of Sound and Vibration* **271** (2004) 453-463.

A The nonlinear force and strain expansions

The quadratic and cubic geometric force operators are

$$\begin{aligned}\mathcal{N}_2(\mathbf{u}, \mathbf{u}) \cdot \mathbf{i} &= [\cos \theta_0 (k - N_0) (e_1^2 - e_2 - e_1 u')]'] \\ \mathcal{N}_2(\mathbf{u}, \mathbf{u}) \cdot \mathbf{j} &= [\cos \theta_0 (k - N_0) (\tan \theta_0 (e_1^2 - e_2) - e_1 v')]'] \\ \mathcal{N}_2(\mathbf{u}, \mathbf{u}) \cdot \mathbf{k} &= [\cos \theta_0 (N_0 - k) w' e_1']\end{aligned}\quad (35)$$

$$\begin{aligned}\mathcal{N}_3(\mathbf{u}, \mathbf{u}, \mathbf{u}) \cdot \mathbf{i} &= [\cos \theta_0 (N_0 - k) (e_1^3 - 2e_1 e_2 + e_3 - e_1^2 u' + e_2 u')]'] \\ \mathcal{N}_3(\mathbf{u}, \mathbf{u}, \mathbf{u}) \cdot \mathbf{j} &= [\cos \theta_0 (N_0 - k) (\tan \theta_0 (e_1^3 - 2e_1 e_2 + e_3) - e_1^2 v' + e_2 v')]'] \\ \mathcal{N}_3(\mathbf{u}, \mathbf{u}, \mathbf{u}) \cdot \mathbf{k} &= [\cos \theta_0 (k - N_0) (e_1^2 - e_2) w']'\end{aligned}\quad (36)$$

The first-, second-, and third-order strains are

$$\begin{aligned}e_1 &= \cos^2 \theta_0 (u' + \tan \theta_0 v') \\ e_2 &= \frac{1}{2} \cos^4 \theta_0 \left[(u' \tan \theta_0 - v')^2 + \frac{w'^2}{\cos^2 \theta_0} \right] \\ e_3 &= -\frac{1}{2} \cos^6 \theta_0 (u' + \tan \theta_0 v') \left[(u' \tan \theta_0 - v')^2 + \frac{w'^2}{\cos^2 \theta_0} \right]\end{aligned}\quad (37)$$

B 2:1 interaction coefficients

The coefficients in Eq. (26) are [11]

$$\begin{aligned}\hat{\Delta}^{(\infty)} &= \frac{1}{8\omega_n} \sum_{j=1}^{\infty} \left[(\Lambda_{nnj} + \Lambda_{njn}) \left(\frac{2\Lambda_{jnn}}{\omega_j^2} + \frac{\Lambda_{jnn}}{\omega_j^2 - 4\omega_n^2} \right) \right] \\ &\quad + \frac{3}{8\omega_n} \Theta_{nnnn} \\ \hat{\Gamma}_{mn}^{(\infty)} &= \sum_{j=1, j \neq m}^{\infty} [(\Lambda_{mjn} + \Lambda_{mnj}) (\Lambda_{jmn} + \Lambda_{jnm}) \\ &\quad \times \left(\frac{1}{\omega_j^2 - 9\omega_m^2} + \frac{1}{\omega_j^2 - \omega_m^2} \right) + \frac{2\Lambda_{jnn}}{\omega_j^2} (\Lambda_{mmj} + \Lambda_{mjm})] \\ &\quad + \frac{(\Lambda_{mnn} + \Lambda_{nmm})^2}{8\omega_m^2} + \frac{4}{\omega_m^2} (\Lambda_{mnn} \Lambda_{mmm}) \\ &\quad + 2(\Theta_{mnnm} + \Theta_{mnmn} + \Theta_{mmnn})\end{aligned}\quad (38)$$

where

$$\Theta_{ijkh} = \int_0^1 \phi_i \cdot \hat{\mathcal{N}}_3(\phi_j, \phi_k, \phi_h) dx \quad (39)$$

Accepted manuscript

List of Figures

1	The geometry of the cable model with the inertial reference frame: \mathcal{C}_0 and \mathcal{C} indicate the initial static and the current dynamic configurations, respectively.	26
2	a) Variation of γ with the sag-to-span ratio d and (b) region of admissible physical nondimensional parameters in the γ - λ plane. The curves indicate iso-stiffness curves: $k_1 = 2.5 \cdot 10^2$ and $k_2 = 5 \cdot 10^4$. Variation of the frequencies of the in-plane modes with $\frac{\lambda}{\pi}$ when (c) $\gamma = 0.75$ and (d) $\gamma = 1.5$. A (S) denotes skew-symmetric (symmetric) modes.	27
3	Variation of $\Gamma^{(\infty)}$, $\hat{\Gamma}^{(\infty)}$ and $\Gamma^{(m)}$ with λ/π of the lowest mode ($m = 1$) when $\gamma = 0.75$.	28
4	Variation of $\Gamma^{(\infty)}$, $\hat{\Gamma}^{(\infty)}$ and $\Gamma^{(m)}$ with λ/π of the third mode ($m = 3$) when $\gamma = 0.75$.	29
5	Variation of $\Gamma^{(\infty)}$, $\hat{\Gamma}^{(\infty)}$ and $\Gamma^{(m)}$ with λ/π of the fifth mode ($m = 5$) when $\gamma = 1.5$.	30
6	Variations of $\Gamma^{(\infty)}$, $\hat{\Gamma}^{(\infty)}$ and $\Gamma^{(m)}$ with λ/π of (a) the seventh mode ($m = 5$) and (b) the seventeenth mode ($m = 17$) when $\gamma = 1.5$.	31
7	Variation of $\Gamma^{(\infty)}$ and $\Gamma^{(m)}$ with λ/π of the lowest elasto-dynamic mode ($m = 17$) of a nonshallow cable ($\gamma = 1.5$).	32
8	The lowest mode (skew-symmetric). First-order (thin line) and second-order (thick) approximations of the displacement field: (a) $u(x)$ and (b) $v(x)$; in part (c) α_k and $(\Phi_1^{(\infty)}, \Phi_2^{(\infty)})$; in part (d) β_k and $(\Psi_1^{(\infty)}, \Psi_2^{(\infty)})$ when $\gamma = 1.5$ and $\lambda = 7\pi$.	33
9	The lowest mode (skew-symmetric): (a) modal coefficient of the softening part of the effective nonlinearity coefficient; (b) convergence of the effective nonlinearity coefficient when when $\gamma = 1.5$ and $\lambda = 7\pi$.	34

- 10 The lowest mode (skew-symmetric). First-order (thin line) and second-order (thick) approximations of the displacement field: (a) $u(x)$ and (b) $v(x)$; in part (c) α_k and $(\Phi_1^{(\infty)}, \Phi_2^{(\infty)})$; in part (d) β_k and (Ψ_1, Ψ_2) when $\gamma = 1.5$ and $\lambda = 12.6\pi$ 35

Accepted manuscript

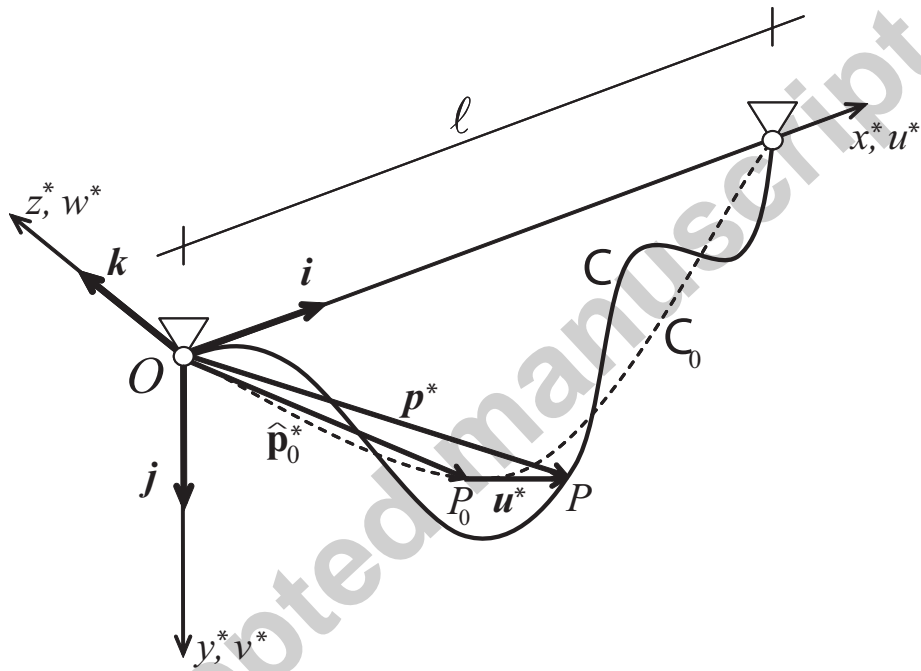


Figure 1: The geometry of the cable model with the inertial reference frame: C_0 and C indicate the initial static and the current dynamic configurations, respectively.

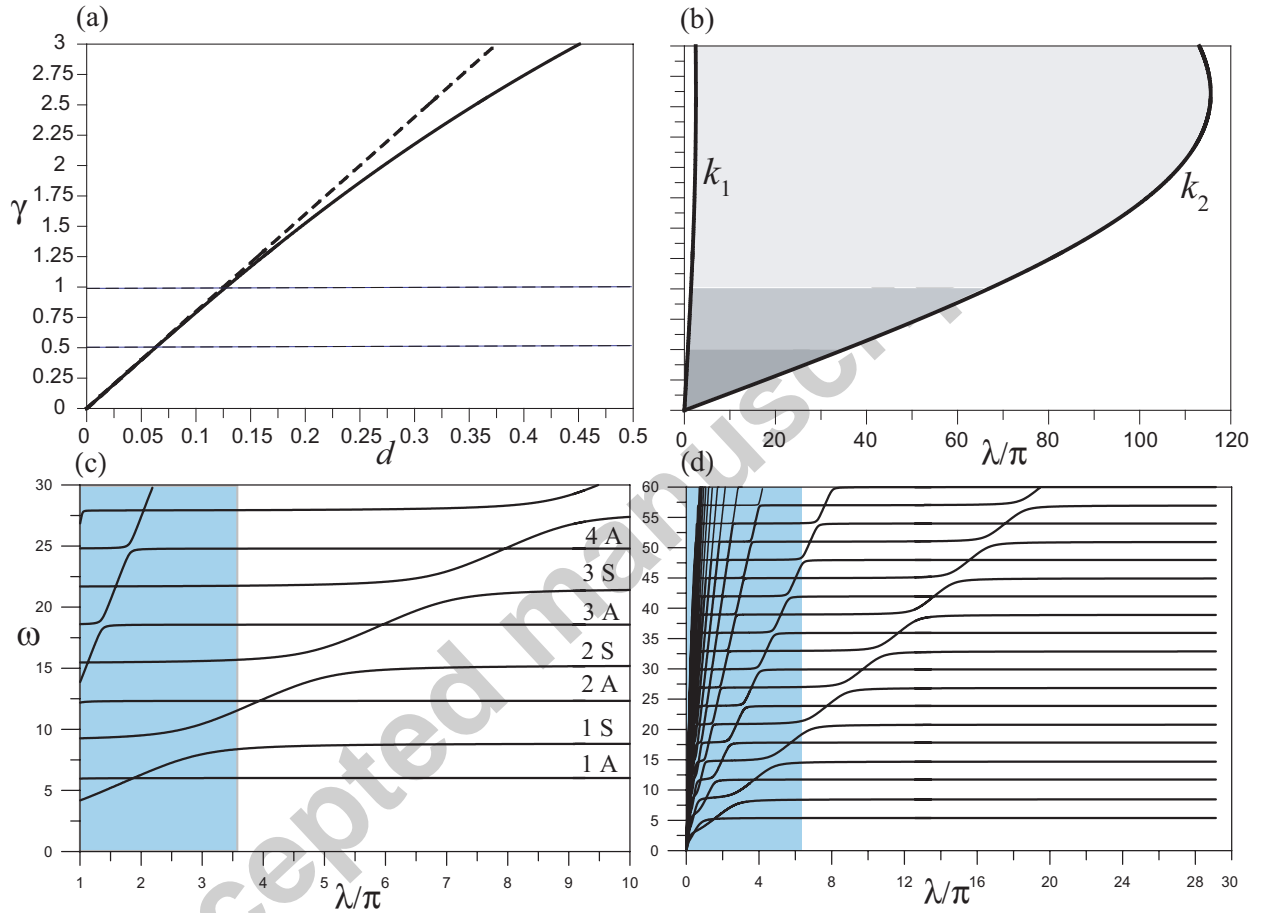


Figure 2: a) Variation of γ with the sag-to-span ratio d and (b) region of admissible physical nondimensional parameters in the γ - λ plane. The curves indicate iso-stiffness curves: $k_1 = 2.5 \cdot 10^2$ and $k_2 = 5 \cdot 10^4$. Variation of the frequencies of the in-plane modes with $\frac{\lambda}{\pi}$ when (c) $\gamma = 0.75$ and (d) $\gamma = 1.5$. A (S) denotes skew-symmetric (symmetric) modes.

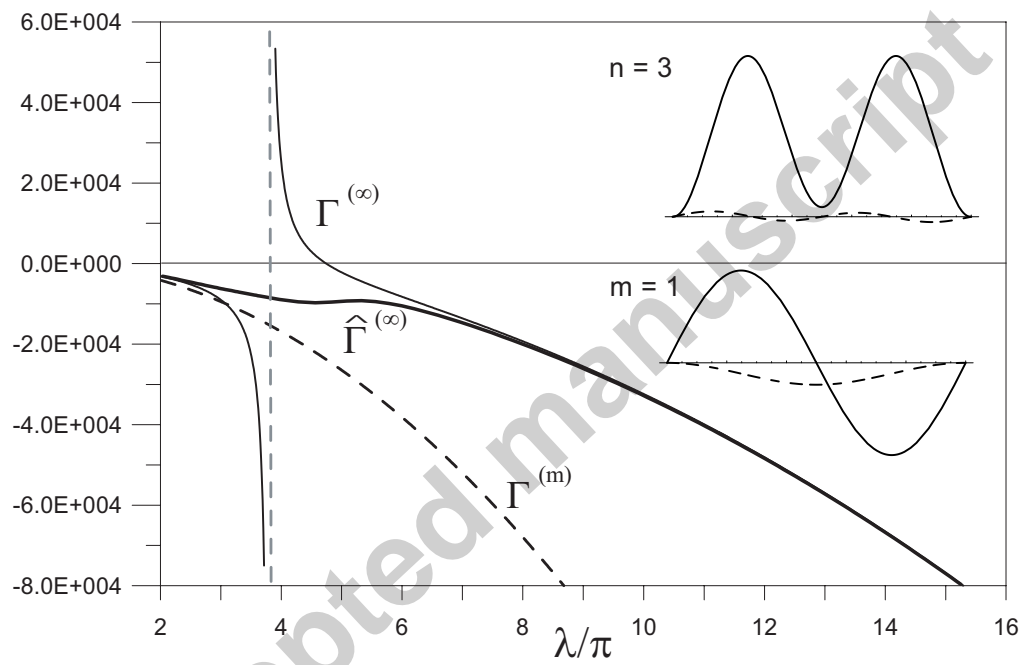


Figure 3: Variation of $\Gamma^{(\infty)}$, $\hat{\Gamma}^{(\infty)}$ and $\Gamma^{(m)}$ with λ/π of the lowest mode ($m = 1$) when $\gamma = 0.75$.

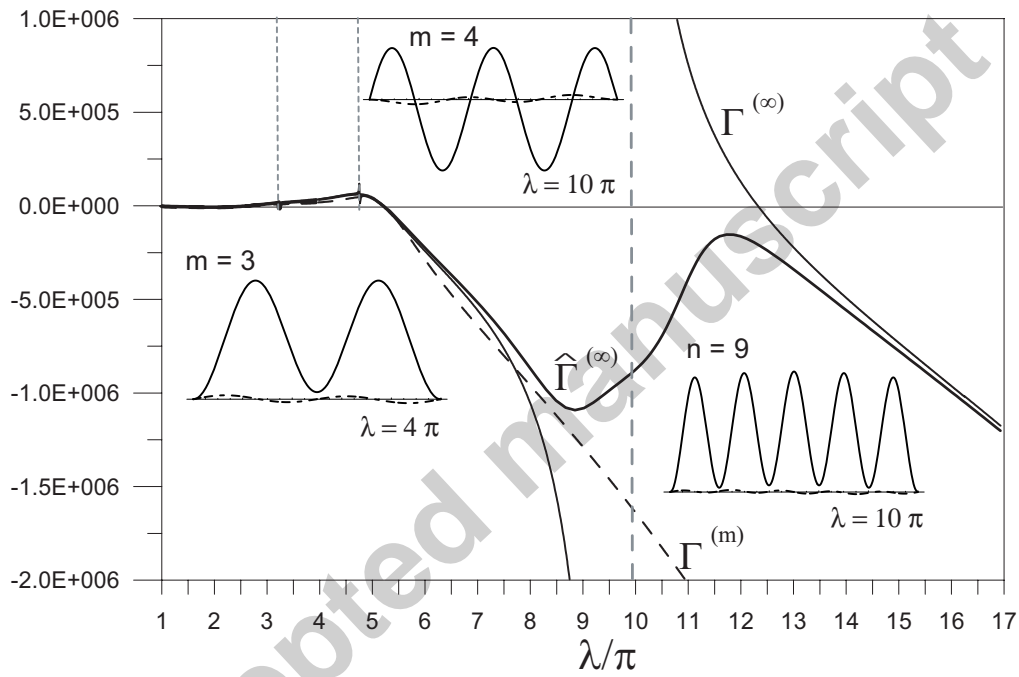


Figure 4: Variation of $\Gamma^{(\infty)}$, $\hat{\Gamma}^{(\infty)}$ and $\Gamma^{(m)}$ with λ/π of the third mode ($m = 3$) when $\gamma = 0.75$.

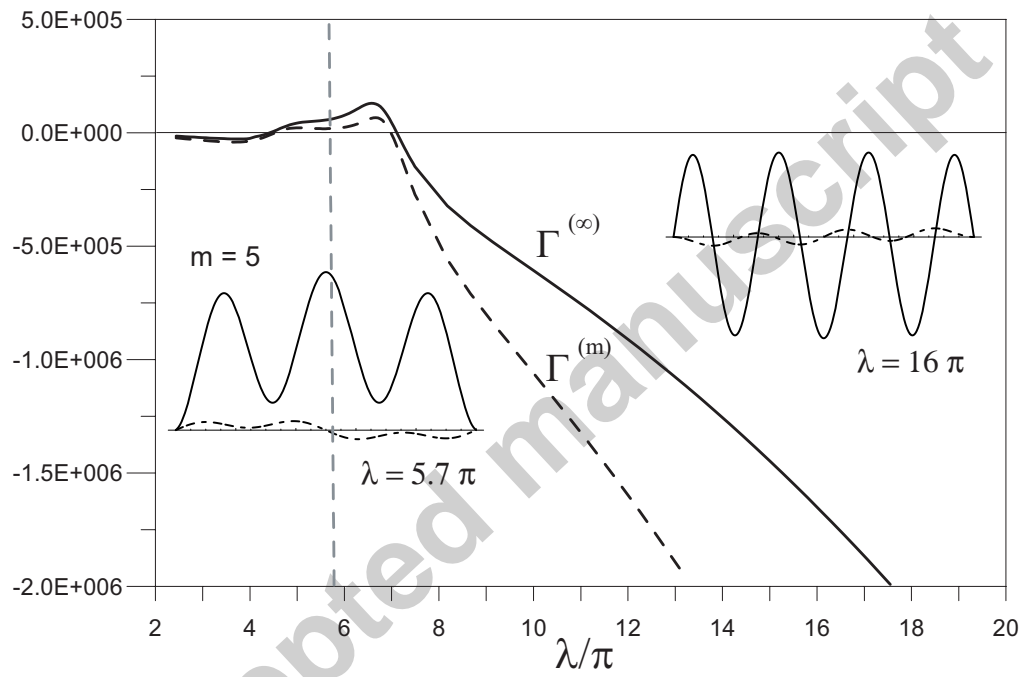


Figure 5: Variation of $\Gamma^{(\infty)}$, $\hat{\Gamma}^{(\infty)}$ and $\Gamma^{(m)}$ with λ/π of the fifth mode ($m = 5$) when $\gamma = 1.5$.

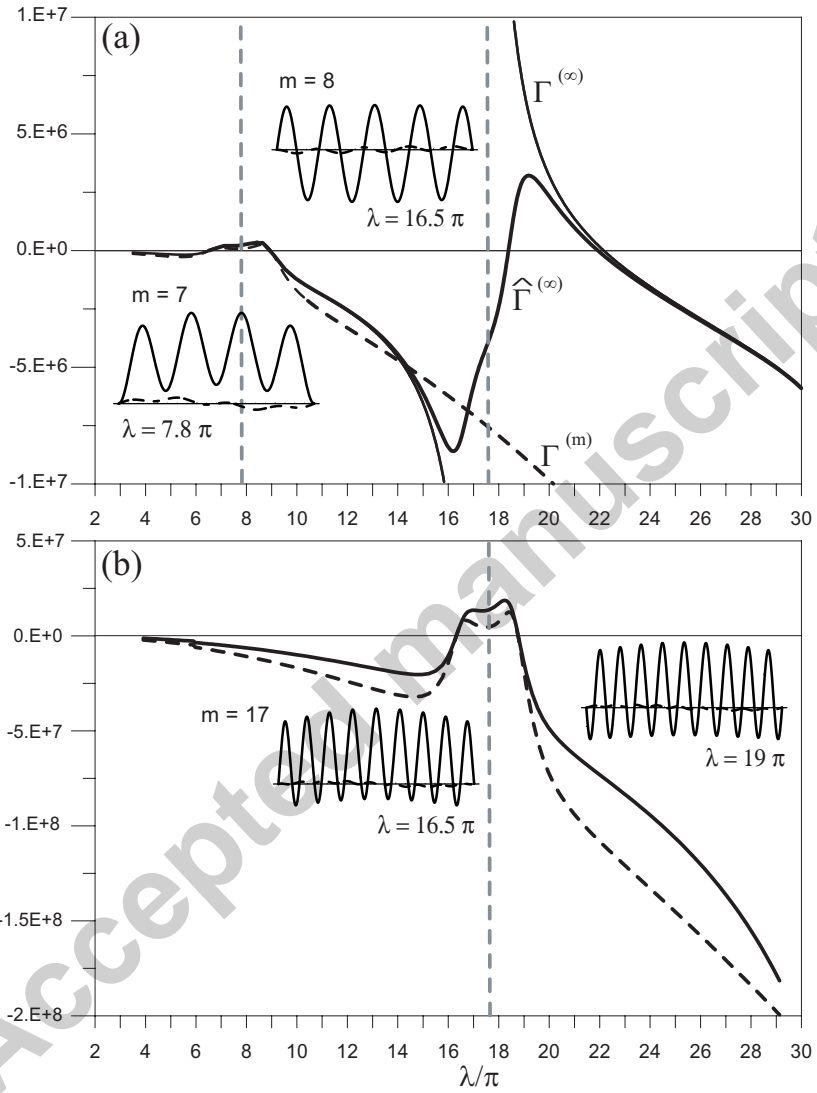


Figure 6: Variations of $\Gamma^{(\infty)}$, $\hat{\Gamma}^{(\infty)}$ and $\Gamma^{(m)}$ with λ/π of (a) the seventh mode ($m = 5$) and (b) the seventeenth mode ($m = 17$) when $\gamma = 1.5$.

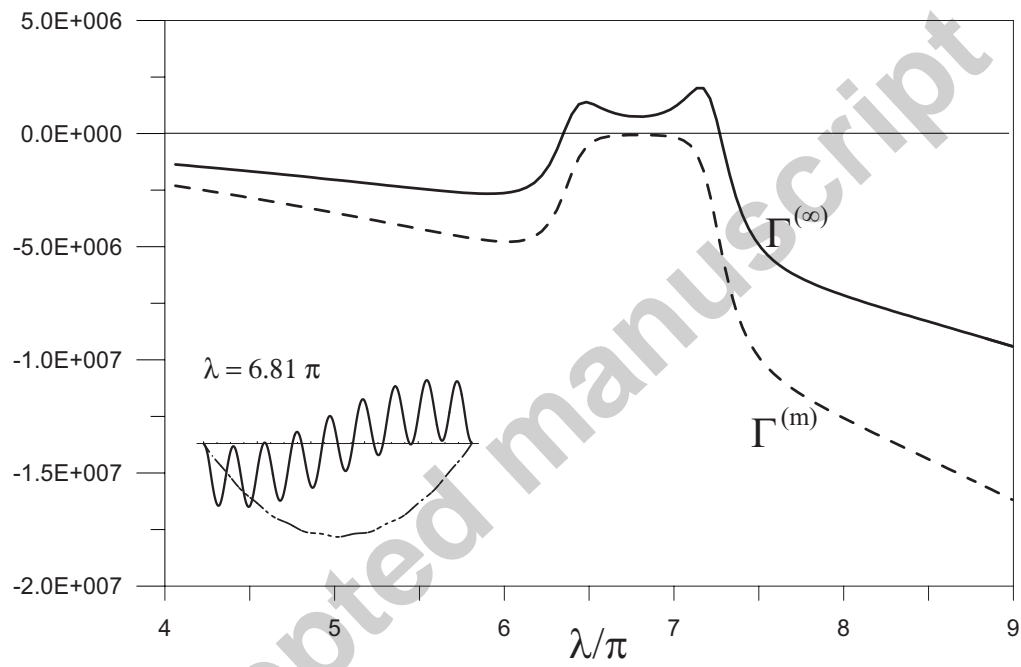


Figure 7: Variation of $\Gamma^{(\infty)}$ and $\Gamma^{(m)}$ with λ/π of the lowest elasto-dynamic mode ($m = 17$) of a nonshallow cable ($\gamma = 1.5$).

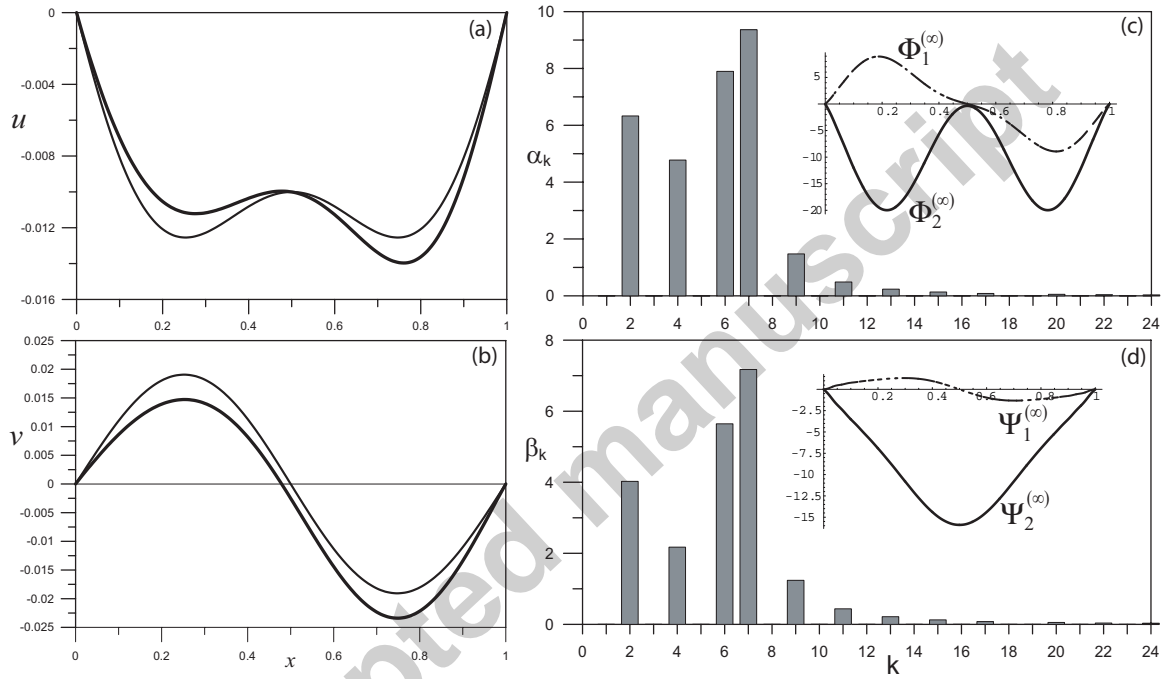


Figure 8: The lowest mode (skew-symmetric). First-order (thin line) and second-order (thick) approximations of the displacement field: (a) $u(x)$ and (b) $v(x)$; in part (c) α_k and $(\Phi_1^{(\infty)}, \Phi_2^{(\infty)})$; in part (d) β_k and $(\Psi_1^{(\infty)}, \Psi_2^{(\infty)})$ when $\gamma = 1.5$ and $\lambda = 7\pi$.

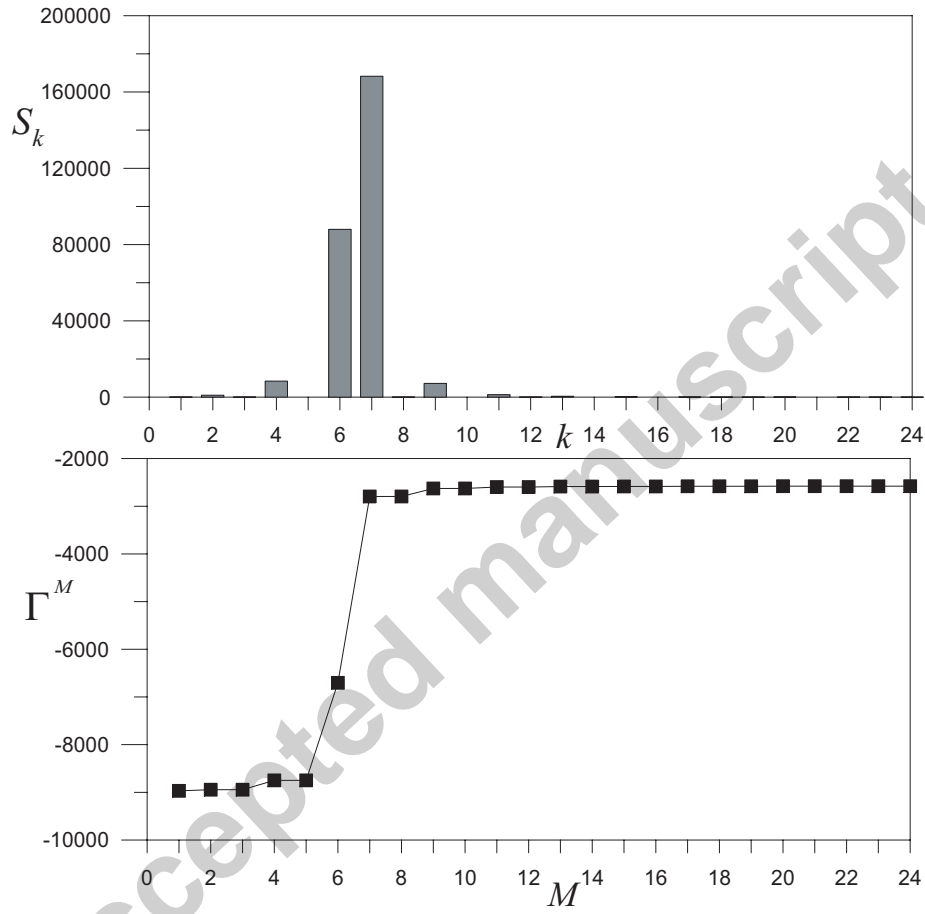


Figure 9: The lowest mode (skew-symmetric): (a) modal coefficient of the softening part of the effective nonlinearity coefficient; (b) convergence of the effective nonlinearity coefficient when $\gamma = 1.5$ and $\lambda = 7\pi$.

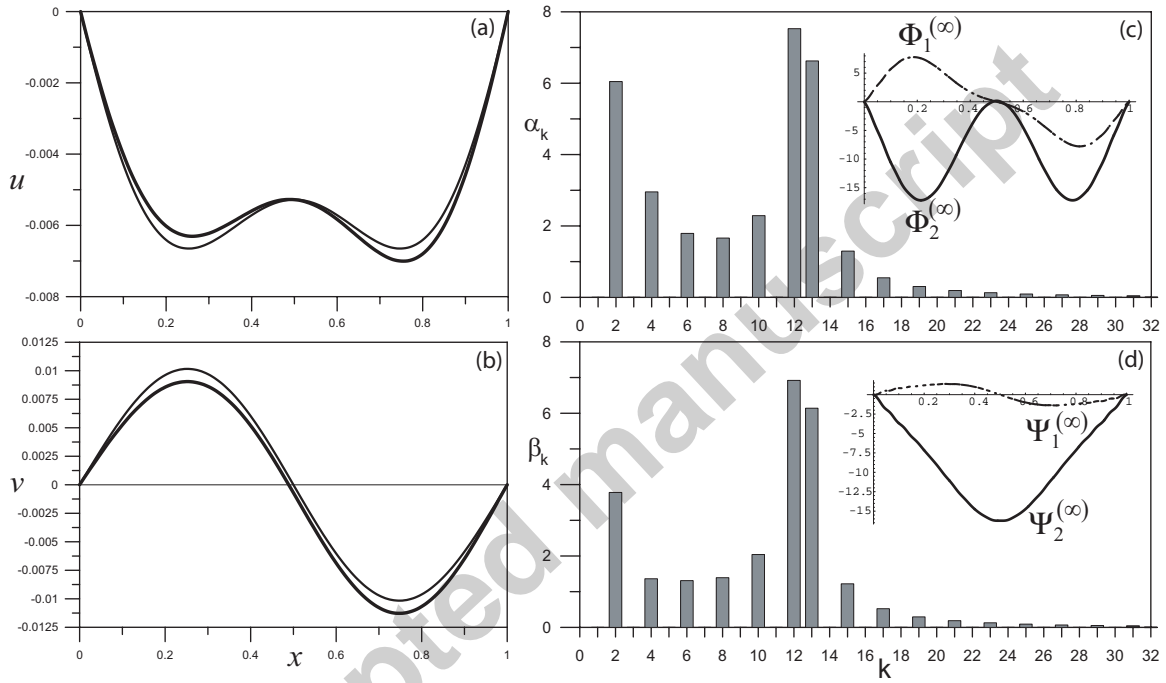


Figure 10: The lowest mode (skew-symmetric). First-order (thin line) and second-order (thick) approximations of the displacement field: (a) $u(x)$ and (b) $v(x)$; in part (c) α_k and $(\Phi_1^{(\infty)}, \Phi_2^{(\infty)})$; in part (d) β_k and (Ψ_1, Ψ_2) when $\gamma = 1.5$ and $\lambda = 12.6\pi$.